PHYSICAL REVIEW A **74**, 053419 (2006)

Spinful bosons in an optical lattice

Sara Bergkvist,[1,*] Ian P. McCulloch,[2] and Anders Rosengren[1]
[1]*Condensed Matter Theory, Physics Department, KTH, AlbaNova University Center, SE-106 91 Stockholm, Sweden*
[2]*Institute for Theoretical Physics C, RWTH Aachen University, D-52056 Aachen, Germany*
(Received 10 June 2006; published 28 November 2006)

We analyze the behavior of cold spin-1 particles with antiferromagnetic interactions in a one-dimensional optical lattice using density matrix renormalization group calculations. Correlation functions and the dimerization are shown and we also present results for the energy gap between ground state and the spin excited states. We confirm the anticipated phase diagram, with Mott-insulating regions of alternating dimerized $S=1$ chains for odd particle density versus on-site singlets for even density. We find no evidence for any additional ordered phases in the physically accessible region, however for sufficiently large spin interaction, on-site singlet pairs dominate leading, for odd density, to a breakdown of the Mott insulator or, for even density, a real-space singlet superfluid.

DOI: 10.1103/PhysRevA.74.053419 PACS number(s): 32.80.Pj, 71.35.Lk

I. INTRODUCTION

Strongly interacting systems which are at the forefront of study in theoretical condensed matter physics can be realized with cold atomic gases in optical lattices. Spinor atoms in optical lattices constitute a novel realization of quantum magnetic systems. These realizations have several advantages compared to their condensed matter counterparts. One is precise knowledge of the underlying microscopic model, another is the possibility to control the parameters of the lattice Hamiltonian, a third is the absence of impurities in the system. Due to the smallness of the scattering length compared to interparticle separation, a gas of degenerate alkali-metal atoms is considered as a weakly interacting gas [1]. However, this is no longer true if the atomic scattering length is changed by means of a Feshbach resonance [2] or if an optical lattice created by standing wave laser beams is used to confine the atoms in the minima of the lattice potential, which strongly enhances the effects of the interactions.

For the case of the optical lattice the Mott insulator-superfluid quantum phase transition was first demonstrated in the seminal experiment of Greiner *et al.* [3] for ^{87}Rb. This experiment has led to an enormous research activity in the field of cold atoms confined in optical lattices. In most experiments on cold atoms a magnetic field is used to create a trap that confines the atoms in the lattice. This means that the spins of the atoms are fully polarized so that the atoms behave as spinless particles. Recently an experimental setup that uses an optical, instead of magnetic, trap has been developed [4,5]. Using this type of confinement atoms with different spin polarizations are trapped and the scattering of the atoms become spin dependent [6–8]. The spin interaction may be either antiferromagnetic or ferromagnetic in its structure depending on the scattering length which is material specific. For sodium ^{23}Na, the interaction is antiferromagnetic [6].

A model for spinful bosons in optical lattices has been studied before by a number of groups [6–13], and a phase diagram has been predicted. For integer number of atoms per lattice site there are two regimes. One, where the kinetic energy is dominating over the potential energy, has a superfluid ground state and the other, where the interaction energy is the most important, has a Mott insulating ground state. For noninteger particle density the superfluid ground state is always prevailing. For the one-dimensional case the predicted phase diagram has a spin-dimerized phase in the insulating regions with odd particle density and on-site spin singlets in the insulating regions with even density. This phase diagram was recently confirmed numerically [14]. However, for the study of the order parameter the authors' resorted to a mapping of the boson model to a spin model [7]. By doing so the dimension of the local Hilbert space is reduced from 20 or more (depending on the maximum number of bosons per site) to three, and accordingly the calculations are less time and memory consuming. However, this mapping is only applicable to the insulating regions with odd density, and is valid in the limit of very strong atom-atom repulsion.

Our aim with this article is to study the spinful model directly. The correlation functions and excitation energies are presented for the first three insulating regions. We also compare results for the insulating systems with those for the superfluid phase. All calculations in this article are done using density matrix renormalization group (DMRG) with open boundary conditions.

The outline of the paper is as follows. In Sec. II the model and the mapping from the spinful Hamiltonian to the spin-one chain is presented. In Sec. III some details about the calculations are given. In Sec. IV we present particle-particle and spin-spin correlation functions for the system. In Sec. V the dimerization in the spin-spin correlation is obtained and from this it is concluded that the third Mott lobe is dimerized and that the first lobe most probably is dimerized. In Sec. VI the energy gap to excited spin states is investigated. It is apparent that the second Mott lobe has on-site singlets and that the gap decays with a universal behavior when the superfluid phase is approached. We also show that the odd density insulating systems have a small spin gap and that this energy gap is nonzero for all spin-interaction strengths. Section VII contains a discussion on the conditions under which bound on-site singlet phases occur. This gives several new states, including a singlet insulator and a superfluid phase of condensed singlet pairs (SSCs) [6,8]. In this latter phase the

*Electronic address: sarber@kth.se

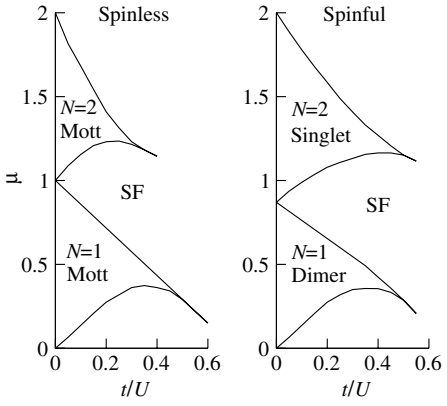

FIG. 1. A sketch of the phase diagram of the Bose-Hubbard model [14]. The left panel shows the Mott lobes for the spinless Bose-Hubbard model and the right panel shows the spinful phase diagram ($J/U=0.1$).

tunneling of individual atoms is suppressed and only singlet pairs tunnel [6]. The last section, Sec. VIII, is devoted to a summary and conclusions.

II. THE MODEL

In most experiments on optical lattices a magnetic trap is used to confine the atoms. Due to the spin dependent interaction between the atoms and the trap only one of the spin species is confined in the lattice. This system is very well described by the Bose-Hubbard model [16]. The phase diagram for the spinless Bose-Hubbard model was discussed in the seminal work by Fisher *et al.* [17] using a scaling theory and renormalization-group calculations. They also derived the exact phase diagram within mean-field theory, i.e., for an infinite-range hopping model. The phase diagram for the one-dimensional model has been obtained numerically with a high precision by Kühner *et al.* [15,18] using the DMRG method. The phase diagram has Mott insulating regions (Mott lobes) and superfluid regions. A sketch of the phase diagram is shown in the left panel of Fig. 1.

When an optical trap is used instead of a magnetic trap, atoms with all spin polarization are trapped, with alkali atoms having hyperfine spin $F=1$. The scattering between two atoms takes place in the spin-zero and the spin-two sectors. Since the scattering length is different in these two sectors the on-site repulsion becomes spin dependent, resulting in the following Hamiltonian [6,7]:

$$H = -t\sum_{i,\sigma}(b^{\dagger}_{i,\sigma}b_{i+1,\sigma} + b_{i,\sigma}b^{\dagger}_{i+1,\sigma}) + \sum_{i}[Un_i(n_i-1) + J\mathbf{S}_i^2]. \tag{1}$$

Here $b^{+}_{i,\sigma}$ and $b_{i,\sigma}$ are the creation and annihilation operators for bosons with the z component of spin $\sigma=0,\pm1$, in the lowest Bloch band localized on site i, $n_i=\Sigma_\sigma b^{+}_{i,\sigma}b_{i,\sigma}$ is the local density, t is the hopping integral for atomic wavefunctions between different lattice sites, U is the usual on-site Coulomb repulsion, $\mathbf{S}_i=\Sigma_{\sigma,\sigma'}b^{+}_{i,\sigma}\mathbf{T}_{\sigma,\sigma'}b_{i+1,\sigma'}$ is the spin operator for spin one particles at lattice site i, with $\mathbf{T}_{\sigma,\sigma'}$ being the usual spin-1 matrices. J is the spin dependent interaction whose value and sign depend on the material. For ^{23}Na, J is positive, i.e., the spin interaction is antiferromagnetic, and $J/U\approx0.04$ [7]. In this paper we focus mainly on the parameter range appropriate for ^{23}Na.

The insulating regions with an odd density form an effective spin-one chain, as the spins on each lattice site will combine to the lowest possible spin. This maps the insulating odd density region for the spinful Bose-Hubbard model onto the bilinear-biquadratic spin-one chain with Hamiltonian [7,8,10,14]

$$H = \sum_{\langle ij\rangle}[\cos\theta(\mathbf{S}_i\cdot\mathbf{S}_j) + \sin\theta(\mathbf{S}_i\cdot\mathbf{S}_j)^2], \tag{2}$$

where $\tan(\theta)=\frac{1}{1-2J/U}$, $\theta\in[-3\pi/4,-\pi/2]$, for the first Mott lobe. Similar expressions should exist for higher (odd) Mott lobes.

The mapping is obtained by making a lowest order, i.e., second order, perturbation expansion in t of the Hamiltonian (1). To second order only pairwise interactions between atoms on neighboring sites are generated. For the first Mott lobe, i.e., in the insulating state with exactly one boson per site, the nearest-neighbor interactions are always of the form given by Eq. (2). However, the derivation of the θ dependence on J and U is only valid in the limit $t\ll U$. Away from the limit $t\ll U$ but still in the insulating phase, higher order terms have to be included which will, in addition to renormalizing the nearest-neighbor couplings, add spin couplings beyond nearest neighbor.

Despite many years of study, the phase diagram of the spin 1 chain is not fully resolved. For $\theta=0$, the antiferromagnetic Heisenberg model, the spectrum has a finite Haldane gap [19], whereas at $\theta=\pm\pi$ the system is ferromagnetic. Actually, both phases have a finite extension in parameter space. Ferromagnetism exists for $-\pi<\theta<-3\pi/4$ and $\pi/2<\theta<\pi$ while the massive Haldane phase exists for $-\pi/4<\theta<\pi/4$. At the lower end of this interval $-\pi/4$ the gap vanishes, but opens again for $\theta<-\pi/4$ and a massive dimerized state with spontaneously broken translation symmetry is found. For the special point $\theta=-\pi/2$, the ground-state energy, gap, correlation length and the dimer order parameter can be calculated exactly [20]. The unresolved issue is whether the dimerized phase extends all the way to $\theta=-3\pi/4$ or if there exists another phase in between the dimerized and the ferromagnetic phase near $\theta=-3\pi/4$.

Chubukov [21], studying fluctuation effects near the end point of the ferromagnetic phase, concluded that the dimerized and the ferromagnetic phase are separated by a disordered phase, a gapped nondimerized nematic. According to Chubukov a direct transition between the dimerized and ferromagnetic phases is very unlikely since completely different symmetries are broken in these phases. Chubukov claimed that the dimer order parameter and the gap vanish simultaneously at a θ_c above, but close to, $\theta=-3\pi/4$. For $\theta<\theta_c$ the gap opens up and closes again at $\theta=-3\pi/4$ whereas the dimer order parameter is zero in this interval. Buchta *et al.* recently performed highly accurate DMRG calculations [22] for this region. Their results indicate that the dimer phase prevails down to $\theta=-3\pi/4$, although they cannot rule out

that a non-dimerized phase exists in an extremely small interval of θ close to $\theta=-3\pi/4$. A recent preprint by Läuchli, Schmid, and Trebst [23], uses a strong-coupling series expansion which gives a vanishing gap for $-3\pi/4<\theta<-0.67\pi$, but they also present DMRG results that are consistent with those of Buchta *et al.* [22] showing a small but finite gap in this region. Porras *et al.* [24] introduced a numerical algorithm and applied it to the same problem. They found indications of a quantum phase characterized by nematic quasi-long-range order in the interval $-3\pi/4<\theta<-0.7\pi$. However, the accuracy of this calculation is difficult to quantify; their results are also consistent with either the correlation length being longer than the size of the chains considered, or a gap that is smaller than the numerical accuracy [24]. Also, Rizzi *et al.* [14] concluded from DMRG calculations that there is no intermediate nematic phase, although they found indications that a tendency towards nematic ordering is enhanced as the dimer order parameter goes to zero.

In the odd density insulating state with more than one boson per site there is an additional constraint in order to arrive at the Hamiltonian (1): configurations with spin on individual sites higher than one have to be neglected. Matrix elements for scattering into such states are of the order $(nt)^2/U$ and their energy is set by J, where n is the number of bosons per site. Therefore in order to obtain the bilinear-biquadratic Hamiltonian, the condition is that $nt \ll (UJ)^{1/2}$ [7].

The insulating regions with an even density behave completely differently compared to those with odd density. For an even number of spins per site, the particles form bound states of singlet pairs resulting in a rather large energy gap to the excited states. Note, however, that unless the spin interaction is very large, the even density superfluid shows no such real-space pairing.

The spin interaction affects the critical interaction strength for the transition from the Mott insulating to the superfluid phase. In the Mott lobes with even particle densities, i.e., the insulating regions with on-site spin singlets, the insulating regions are stabilized by the spin interaction. On the other hand the Mott lobes with an odd density are weakened by the spin interaction, the density fluctuation is enhanced since the particle hopping is the process that carries the spin-interaction [25]. In the right panel of Fig. 1 a sketch of the new phase diagram is shown together with the phase diagram for the spinless model (left panel).

III. METHOD

The method we have used is the density matrix renormalization group [26,27], adapted to exactly handle the non-Abelian SU(2) symmetry [28]. The starting point of this formulation is the Wigner-Eckart theorem [29], which states that the matrix elements of SU(2)-invariant operators factorize into a component that is *independent* of the geometry (i.e., the quantization axis), and a geometrical factor (Clebsch-Gordan coefficient). In particular, we have the relationship

$$\langle j'm'|A_M^{[k]}|jm\rangle = C^{j\ k\ j'}_{mMm'} \times \langle j'||\mathbf{A}^{[k]}||j\rangle, \tag{3}$$

where $\langle j'\|\mathbf{A}^{[k]}\|j\rangle$ is the reduced matrix element of the rank k tensor $\mathbf{A}^{[k]}$. From this relation, all of the operations required for the DMRG (tensor products, wave function transformations etc.), can be written in terms of the reduced matrix elements only, with an appropriate $6j$ or $9j$ coupling coefficient [28,29].

The use of symmetries to improve the efficiency of DMRG calculations was recognized from the beginning [26], and presumably arose from the Wilson's use of spin in NRG [30], the historical forerunner of DMRG. The utility of Abelian symmetries [typically U(1), such as particle number, or z component of spin], is that it imposes a sparseness constraint on the operator matrix elements; given a basis labeled by the particle number, for example, the matrix elements of some irreducible operator $\langle n'|A^{[N]}|n\rangle$ are nonzero only for $n'=n+N$. By storing only the matrix elements that are permitted by symmetry to be nonzero, the memory use and computational cost is greatly improved. Note, however, that *a priori* this has no effect on the accuracy, and in principle for a given basis size the obtained matrix elements and wave function will be identical whether the symmetry constraint is used or not. This is in contrast to the case of non-Abelian symmetries, where Eq. (3) implies a reduction in the basis size needed to represent the Hamiltonian matrix elements. That is, a single basis state of total spin j requires $2j+1$ states to represent in a U(1) basis. This results in a proportional reduction in the basis size m required for a given accuracy. Depending on the spin of the block basis states this reduction factor typically ranges from around 3 in the Mott insulating phase where the block spins tend to be minimal, to 8 or so in the superfluid phase. Since the computational cost of the algorithm is proportional to m^3, this results in orders of magnitude improvement in the efficiency.

For these calculations, we typically used 350 basis states [equivalent to approximately 1000–2500 basis states of a U(1) calculation]. For the finite size scaling analyses we used up to 300 lattice sites for the phases with total number of bosons N equal to the number of lattice sites L, up to 120 sites for $N=3L$ and up to 70 sites for the $N=2L$ superfluid. We fixed the maximum number of bosons per site to be 5, except for the $N=L$ superfluid where we found four bosons per site to be sufficient, and the $N=L$ insulator where we found 3 bosons per site to be sufficient. This is justified by the occupation number shown in Fig. 2 where the average number of bosons in the different single site basis states are shown.

IV. CORRELATION FUNCTIONS

In this section we discuss the calculated hopping correlation functions and the spin-spin correlation functions. In the superfluid the hopping correlation function $\Gamma(j)=\langle b^+_{i,\sigma}b_{i+j,\sigma}\rangle$ decays with a power-law as we expect [17]. The low-energy physics of the superfluid phase is described by a Luttinger liquid and the decay of the hopping correlation function $\Gamma(j)\sim j^{-K/2}$ where K is the Luttinger liquid parameter [31]. Since we use open boundary conditions, measures have to be

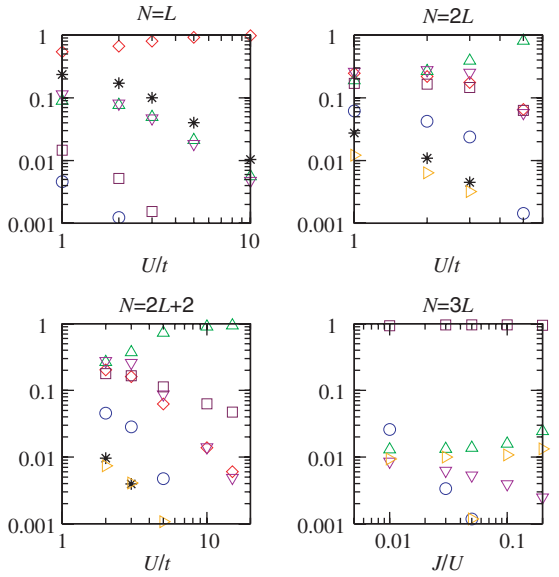

FIG. 2. (Color online) The population of the single-site basis states for an average density of one, two, $N=2L+2$, and three particles. The probability for the different sectors is presented as a function of the on-site repulsion U/t, for $J/U=0.05$, in the first three panels. The last panel shows the third Mott lobe as a function of J/U, with $U/t=15$. The different sectors (n,S) presented in the figure are star (0,0), diamond (1,1), up triangle (2,0), down triangle (2,2), square (3,1), circle (3,3), right triangle (4,0).

taken to reduce the effects of the boundary. The most important effect is oscillations in the local density. In the superfluid phase they show the characteristic Luttinger liquid power-law decay away from the edge of the system. These density fluctuations will affect the hopping correlation function $\Gamma(j)$. Since we are interested in the properties of the infinite system we reduce the effects of these fluctuations by averaging over pairs of $\langle b^+_{i,\sigma} b_{i+j,\sigma}\rangle$ for fixed j. We discard contribution from the ten lattice sites closest to the boundary where the Friedel oscillations are largest. Beyond this distance the numerical behavior of Γ is no longer sensitive to the boundary oscillations. The right panel of Fig. 3 shows results for the hopping correlation function for two different integer densities displaying superfluid behavior.

In the Mott insulating phase the hopping correlation function $\Gamma(j)$ is decaying exponentially [17], where the decay rate is determined by how close we are to the phase boundary of the Mott phase. As one would expect, the boundary effects decay exponentially in this region. The left panel of Fig. 3 shows results for the hopping correlation function for three different integer densities.

In Fig. 4 the spin-spin correlation functions for different systems are presented for Mott insulating and superfluid regions. The spin interaction strength is set to $J/U=0.05$. The figure demonstrates that the correlation function is rather independent of the phase for the odd density systems. It decays in the same way for all the odd density systems and also for the superfluid system with an even density. The insulating system with a density of three atoms per site is dimerized, for this interaction strength, which is the reason for the oscillating structure of the spin-spin correlation.

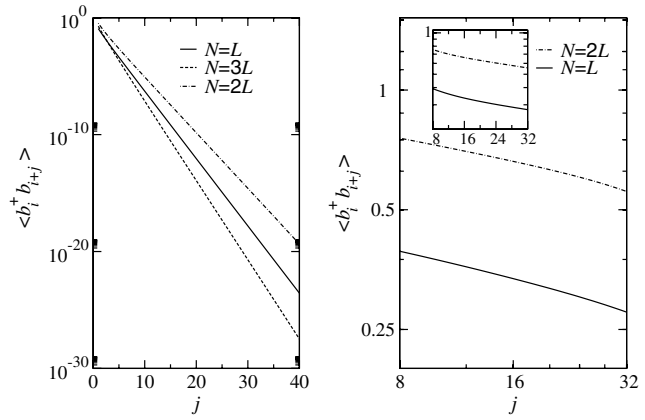

FIG. 3. The $\langle b^+ b\rangle$-correlation function. The left hand panel is in the insulating regime ($U/t=10$, $U/t=10$, $U/t=15$ for $N=L$, $N=2L$, $N=3L$, respectively), the right hand panel shows the superfluid ($U/t=1$ for both $N=L$ and $N=2L$), log-log plot. Inset: same data with a log-linear scale. We fix $J/U=0.05$ in all cases.

For the insulating system with an even density the spin-spin correlation is exponentially decaying, consistent with the picture of on-site singlets.

V. DIMERIZATION

One of the questions that we try to resolve in this article is the nature of the spin order in the first Mott lobe. The phase is, as mentioned above in Sec. II, believed to be dimerized. The standard way to characterize the dimerization is by using a dimer order parameter which usually is defined as the difference in bond energy in the middle of the chain

$$D = \langle H_{j,j+1}\rangle - \langle H_{j-1,j}\rangle. \tag{4}$$

In the spinful Bose-Hubbard model this dimer order parameter is given by $\langle b_j^+ b_{j+1} - b_{j-1}^+ b_j\rangle$ since all other terms in the Hamiltonian are on site. This difference is very difficult to measure since it is very small, see Fig. 5. The figure shows

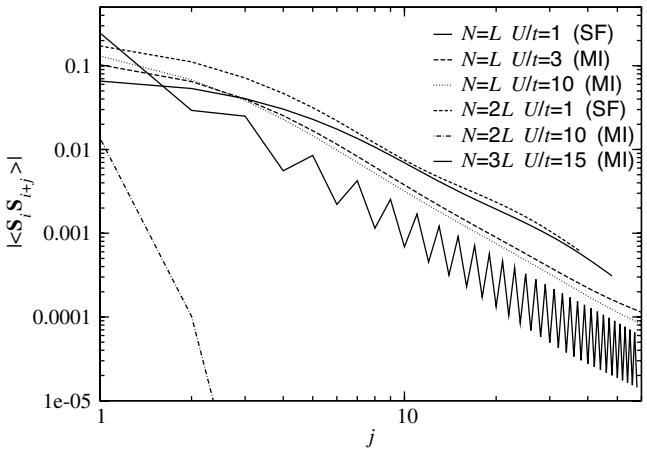

FIG. 4. The spin-spin correlation for $N=L$, both insulating and superfluid, $N=2L$ both insulating and superfluid and $N=3L$ insulating, $J/U=0.05$. The clear oscillation in the correlation function for the third Mott lobe arises from the large dimerization.

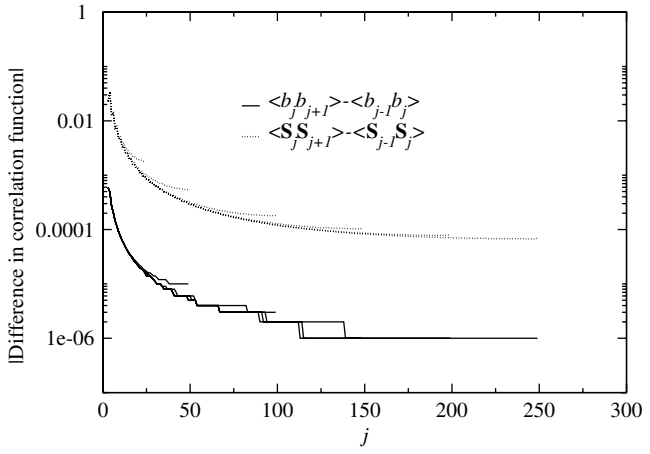

FIG. 5. The absolute value of the difference in neighboring correlation functions in the first Mott lobe ($U/t=10$, $J/t=0.5$) for different system sizes. The dimerization is calculated up to the middle of the chain.

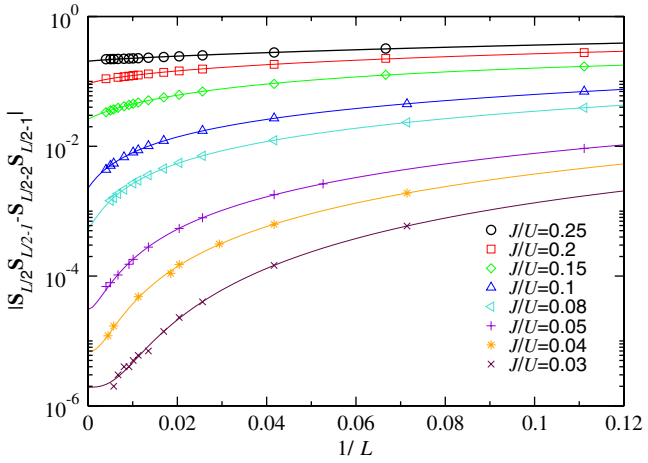

FIG. 6. (Color online) The dimerization in the spin-spin correlation function as a function of the inverse lattice size for the first Mott lobe ($U/t=10$), for different strength of the spin interaction. The solid lines are the finite size scaling.

the absolute value of the mentioned difference as a function of the lattice site j for a Mott insulating system. In the figure j runs between 1 and the middle of the chain. The dimerization is calculated for a couple of different system sizes to illustrate the boundary effects. The bond energy is indeed oscillating between different lattice sites but the values are so small that it is difficult to tell whether or not the oscillation will be nonzero in the thermodynamic limit. The open boundary conditions break the translational symmetry which is necessary to see a dimerized order parameter. For periodic boundary conditions the ground state would be a linear combination of the two possible degenerate dimerized configurations and translational symmetry would be restored for any finite L.

The dimerization in the spin-spin correlation functions for the Mott insulating system has also been studied, the result is presented in Fig. 5. In this figure the dimerization in the spin-spin correlation is shown as a function of the lattice site, for a few system sizes.

The dimerization in the spin-spin interaction for different interaction strengths in the first Mott lobe is shown in Fig. 6. In the figure the spin-spin dimerization at the middle of the lattice is shown as a function of the system size. There is a dimerization when the spin interaction becomes large but it is hard to draw any conclusions about the thermodynamic limit for small interaction strengths. We have done a finite size scaling of the points with the following fitting function [22]

$$D = D_0 + dN^{-\beta} \exp(-N/2\xi). \tag{5}$$

The infinite size values for the first Mott lobe are presented in Fig. 7. The dimerization goes to zero algebraically with an exponent ~ 6, i.e., $D_0 \propto (J/U)^6$. This is in agreement with a calculation on the bilinear biquadratic chain [14]. The curve shows no indication of a nonzero dimerization before $J=0$. The values in the figure are obtained for $U/t=10$ and for $U/t=3$. The fact that the curves for $U/t=3$ and $U/t=10$ fall on top of each other shows that the dimerization is present in the entire Mott lobe. This conclusion cannot be deduced from the bilinear-biquadratic chain, since the mapping is only valid for small hopping.

In Fig. 7 the dimerization in the spin-spin correlation for the third Mott lobe as a function of spin interaction strength is also shown. The values are infinite size values obtained in the same manner as for the first Mott lobe. However, the system sizes are smaller so the error in finite size scaling is larger. As was mentioned in Sec. II also for the third Mott lobe the spinful Bose-Hubbard model could be approximately mapped to the bilinear-biquadratic spin chain. However, in this case the constraints for the perturbation expansion in t to be valid are more severe, configurations with spin on individual sites higher than one have to be neglected leading to the condition $nt \ll (UJ)^{1/2}$. For the dimerization in the third Mott lobe presented in Fig. 7 this condition reads $J/U \gg 0.04$. As configuations with spin higher than one come

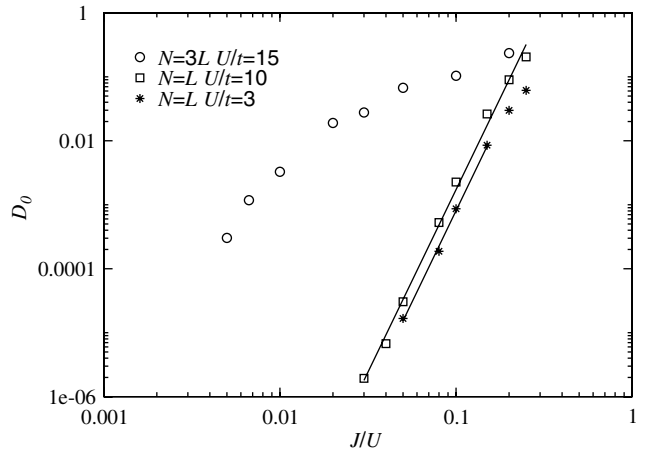

FIG. 7. The dimerization in the thermodynamic limit as a function of spin interaction strength. The dimerization in the first Mott lobe decays algebraically with a fitted exponent ~ 5.7 and there is no suggestion that it will be non zero before $J/U=0$. In the third Mott lobe the dimerization is much larger.

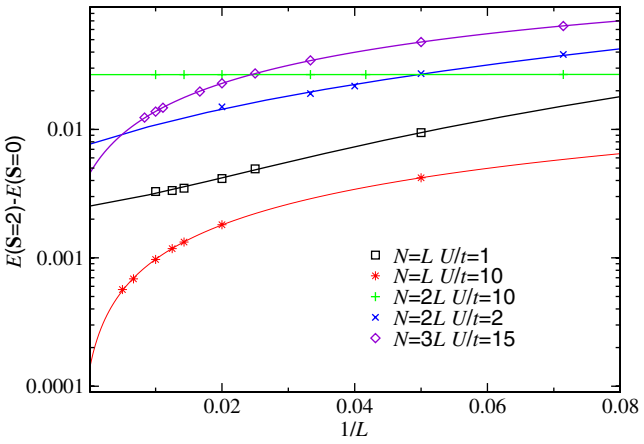

FIG. 8. (Color online) The difference in energy between states $S=2$ and the ground state, $S=0$, as a function of the inverse system size for $J/U=0.05$. The values for the second Mott lobe (denoted "+") are scaled by $1/100$.

into play we see a possible cross over in the behavior and a down turn in the curve for D_0 for $J \leqslant 0.01$. However, still we find no indications of D_0 being zero for J larger than zero. The third Mott lobe is definitely dimerized for $J/U=0.005$ and we conclude that there is no extra phase between the dimerized phase and the ferromagnetic in the third Mott lobe.

VI. SPIN GAPS

In this section, the difference in energy between the ground state, which is a spin singlet, and the first excited spin state, which has spin $S=2$, is studied. This difference is calculated for several system sizes and is shown as a function of the inverse system size in Fig. 8. The energy gap to excited states in the first Mott lobe has been calculated before with DMRG using the mapping to the bilinear-biquadratic spin chain [14] and also in the limit of zero hopping [32].

From the figure it is obvious that the decay of the energy gap, with respect to the inverse system size, for the Mott insulating state with two particles per site behaves differently to that of the other cases. The gap is large which is consistent with the on-site-singlet picture and approaches the thermodynamic limit as L^{-2} [32].

We have studied how the energy gap in the thermodynamic limit for the second Mott lobe approaches the superfluid value as the on-site repulsion U is decreased. The result is shown in Fig. 9, for $J/U=0.05$, $J/U=0.1$, and $J/U=0.15$. To obtain the values in the figure calculations are done for different interaction strengths and system sizes. The infinite size values are found by fitting second-order polynomials to the data points. In the figure the infinite size values are presented as a function of the on-site repulsion for three different strengths of the spin-spin interaction. In the right panel of Fig. 9 the abscissa (U/t) of two of the curves in the left panel has been shifted by a constant $(\Delta_{U/t})$, different for each of them, to show that the curves can be collapsed on top of each other. From this it is clear that the energy gap decays in the same manner for the three interaction strengths when the superfluid phase is approached.

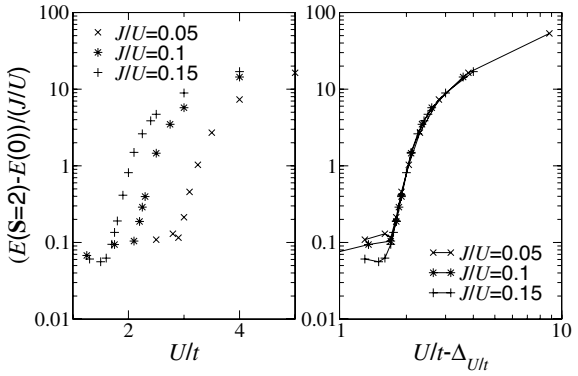

FIG. 9. The spin gap in the thermodynamic limit for the second Mott lobe. In the left panel the values are shown as a function U/t. In the right panel the lines are shifted by a constant $\Delta_{U/t}$ along the x axis to show the similarity in the decay of the gap for the different interaction strengths.

We have further studied how the gap approaches zero for the odd density insulating regions when J/U approaches zero. In Fig. 10, we show for the first Mott lobe at $U/t=10$, the gap as a function of system size, for a variety of different spin couplings. The symbols mark the numerical data and solid lines show the extrapolation to the thermodynamic limit using a second order polynomial fit in $1/L$.

In the first Mott lobe the gap in the thermodynamic limit is very small and decays to zero as the interaction approaches zero, see Fig. 11. In the figure, results for $U/t=10$, i.e., far inside the Mott lobe, are shown together with values for $U/t=3$ which is fairly close to the phase transition. Results for the third Mott lobe and the superfluid phase are also shown in the figure. There is no indication that the energy gap becomes zero before $J=0$. The four curves in Fig. 10 can best be fitted with a power law decay and nothing suggests an intermediate phase in between the dimerized phase and the $J<0$ ferromagnetic phase.

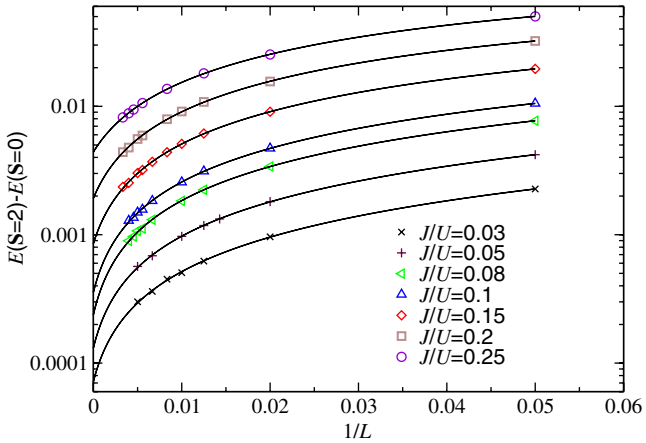

FIG. 10. (Color online) The difference in energy between states with $S=2$ and the ground state, $S=0$, as a function of the inverse system size for $U/t=10$ and different spin interaction strengths the solid lines are finite size scalings.

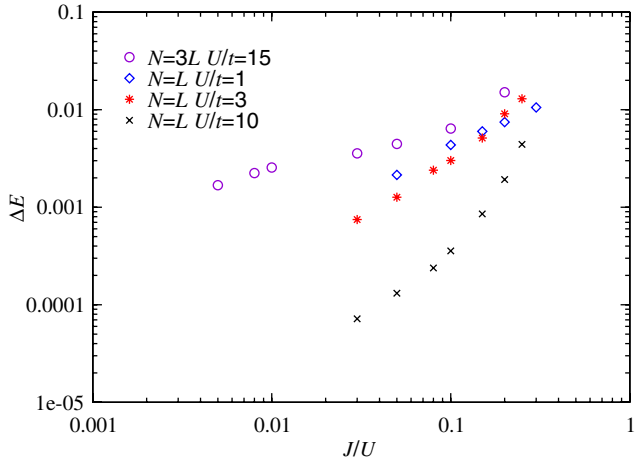

FIG. 11. (Color online) The energy gap between the ground state and the first spin excited state in the thermodynamic limit, as a function of the spin interaction for odd density systems. The system with $U/t=1$ is superfluid.

In Fig. 12 we show the energy per site as a function of the magnetization. We show examples for both insulating and superfluid systems. The spin excitation spectra for the first and the third Mott lobe and the superfluid regions follow the parabolic form typical of Heisenberg spin systems [33]

$$E(S) = E_0 + kS(S+1). \tag{6}$$

The behavior of the spin excitations for the second Mott lobe is rather different, see Fig. 12. In this case, the energy increases linearly with S and with a steep slope, a result which is consistent with the picture of the system being composed of on-site singlets. The energy to break another singlet is independent of the number of already broken singlets. The energy gap to excited spin states measures the magnetization energy and as expected from the on-site singlet picture the second Mott lobe has a higher magnetization energy.

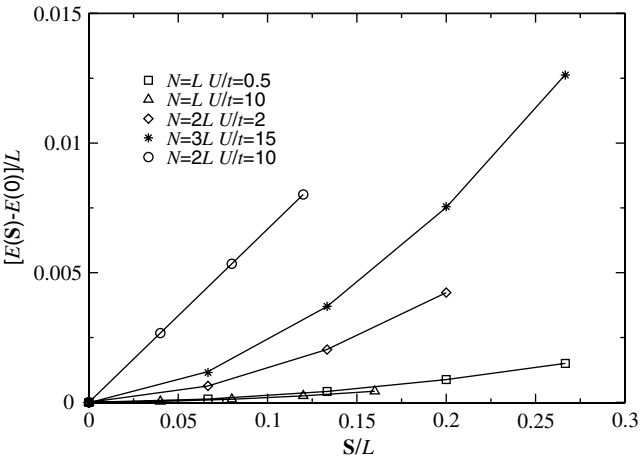

FIG. 12. The energy density as a function of the magnetization $M=S/L$. The open circles for the second Mott lobe have been scaled by a factor 20 to fit on the figure. The fit for these points is a straight line. All other fits are of the form $E_0+kS(S+1)$, $J/U=0.05$.

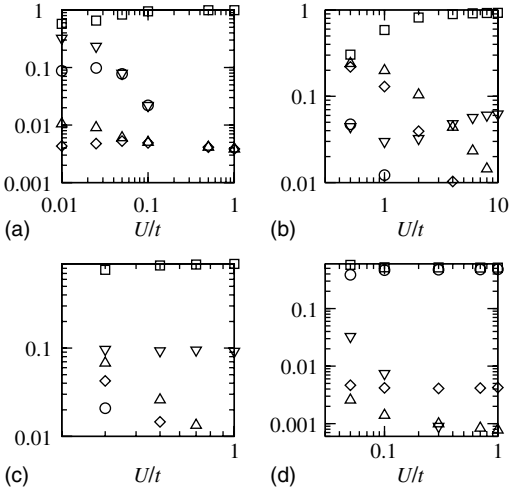

FIG. 13. The probability to have a certain number of particles and spin on a lattice site is presented for different systems and different density and spin (n,S) sectors, circle (0,0), diamond (1,1), square (2,0), up triangle (3,1), down triangle (4,0). (a) $N=2L$ and $J/t=10$: once U and t are comparable in size a singlet condensate forms. (b) $N=2L$ and $J/U=1$: for large U this is an insulating spin-singlet state, seen from the comparatively high probability in the $n=4$ sector. (c) $N=2L+2$ and $J/U=10$: spin singlet condensate. (d) $N=L$ and $J/t=10$: in this spin singlet condensate the lattice is half filled with spin singlets.

VII. SINGLET CONDENSATES

In this section we comment on some of the proposed phases for the spinful Hubbard model. Zhou and Snoek have suggested that a phase exists in between the superfluid and the Mott insulating phases for even particle density [8]. In this hypothesized phase, the particles would form a condensate of tightly bound on-site singlet pairs. However, we see no evidence for this phase for any physically realistic magnitude of spin interaction. In Fig. 2, we show the occupation of each site basis state, for $J/U=0.05$. For this value of the spin interaction, it is clear that there are no values of the Coulomb repulsion U where only even number of bosons is favored. This also follows from a simple energy argument, that suggests such a phase is unlikely: Since the spin interaction energy is smaller than the charging energy it is costly to increase the density on a site by two. The energy gain by keeping the spins coupled to a singlet is much smaller than the energy penalty for the on-site Coulomb repulsion.

For large coupling the system behaves similarly to a spinless Bose-Hubbard model populated with spin singlets. This limit is tested and indeed for $J/t=10$ and $N=L$ the system is essentially composed of $L/2$ empty sites and $L/2$ double occupied sites, see Fig. 13. The limit $J \gg U,t$ could localize the singlets to give a crystal phase [6], but we have not investigated this scenario. In this figure we also show, as a function of U, the population in the different on-site number and spin sectors for $N=2L$ particles per site for the spin interaction strength $J/t=10$, and also the superfluid system with $N=2L+2$ for $J/U=10$. As J/U is reduced, the charging energy becomes equal to the spin energy and the singlets are no longer bound.

VIII. CONCLUSION

We have studied the 1D spinful Bose-Hubbard model using DMRG. By examining the energy and correlation functions we have resolved the behavior of the model for all of the parameter ranges that are physically relevant for optical trapping experiments.

Much evidence is presented showing that the insulating system with an even density is well described by the on-site spin-singlet picture. The spin gap in the thermodynamic limit is rather large, paired with a short correlation length for the spin-spin correlation function. The energy increases linearly with the spin of the system, showing that the energy required to break another singlet is given by the energy gap and is independent of the number of already broken singlets, thus the singlets are strongly localized.

It has been more difficult to determine the nature of the other insulating regions. From the particle-particle correlation function it is concluded that there is a superfluid and an insulating phase just as for the spinless case. It has previously been suggested that these insulating regions are dimerized. The dimer order parameter which uses differences in bond energy is difficult to measure in numerical simulations since it is rather small. Instead the oscillations in the nearest neighbor spin-spin correlation were used to show that it is likely that the odd density per site Mott lobes are always dimerized. This is a relatively strong result for the third Mott lobe, where the dimerization order parameter is quite large. For the first Mott lobe our results are consistent with the $S=1$ Heisenberg calculations of Buchta *et al.* [22] and Rizzi *et al.* [14]. In general the numerical accuracy of calculations in this regime will be much better for the Heisenberg model compared with the spinful Bose-Hubbard model, so our result does not contribute substantially to the argument over the absence (or otherwise) of the Chubukov nematic phase. However what is clear is that the dimerization in the first Mott lobe shows scaling behavior with an exponent ~ 6 throughout the entire Mott lobe. We found no evidence for novel superfluid phases; in particular the on-site paired superfluid suggested by Zhou and Snoek [8] is absent in this model. The energy gaps to spin excited states were studied, showing that the odd density (superfluid and insulating) and even density superfluid phase follow the form of a parabolic spectrum, proportional to $S(S+1)$.

ACKNOWLEDGMENTS

S.B. is grateful to U. Schollwöck and W. Hofstetter for fruitful discussions and hospitality. This work was supported by the Göran Gustafsson foundation and the Swedish Research Council.

[1] C. Pethick and H. Smith, *Bose-Einstein Condensation in Dilute Gases* (Cambridge University Press, Cambridge, UK, 2002).
[2] K. Burnett, P. S. Julienne, P. D. Lett, E. Tiesinga, and C. J. Williams, Nature (London) **416**, 225 (2002).
[3] M. Greiner, O. Mandel, T. Esslinger, T. W. Hänsch, and I. Bloch, Nature (London) **415**, 39 (2002).
[4] A. Widera, F. Gerbier, S. Folling, T. Gericke, O. Mandel, and I. Bloch, Phys. Rev. Lett. **95**, 190405 (2005).
[5] F. Gerbier, S. Folling, A. Widera, O. Mandel, and I. Bloch, Phys. Rev. Lett. **96**, 090401 (2006).
[6] E. Demler and F. Zhou, Phys. Rev. Lett. **88**, 163001 (2002).
[7] A. Imambekov, M. Lukin, and E. Demler, Phys. Rev. A **68**, 063602 (2003).
[8] F. Zhou and M. Snoek, Ann. Phys. (N.Y.) **308**, 692 (2003).
[9] M. Snoek and F. Zhou, Phys. Rev. B **69**, 094410 (2004).
[10] S. K. Yip, Phys. Rev. Lett. **90**, 250402 (2003).
[11] T. Kimura, S. Tsuchiya, M. Yamashita, and S. Kurihara, cond-mat/0506466 (unpublished).
[12] A. Imambekov, M. Lukin, and E. Demler, Phys. Rev. Lett. **93**, 120405 (2004).
[13] F. Zhou, M. Snoek, J. Wiemer, and I. Affleck, Phys. Rev. B **70**, 184434 (2004).
[14] M. Rizzi, D. Rossini, G. De Chiara, S. Montangero, and R. Fazio, Phys. Rev. Lett. **95**, 240404 (2005).
[15] T. D. Kühner and H. Monien, Phys. Rev. B **58**, R14741 (1998).
[16] D. Jaksch, C. Bruder, J. I. Cirac, C. W. Gardiner, and P. Zoller, Phys. Rev. Lett. **81**, 3108 (1998).
[17] M. P. A. Fisher, P. B. Weichman, G. Grinstein, and D. S. Fisher, Phys. Rev. B **40**, 546 (1989).
[18] T. D. Kühner, S. R. White, and H. Monien, Phys. Rev. B **61**, 12474 (2000).
[19] F. Haldane, Phys. Lett. **93A**, 464 (1983).
[20] J. Parkinson, J. Phys. C **20**, L1029 (1988); M. N. Barber and M. T. Batchelor, Phys. Rev. B **40**, 4621 (1989); A. Klümper, Europhys. Lett. **9**, 815 (1990); Y. Xian, Phys. Lett. A **183**, 437 (1993).
[21] A. V. Chubukov, Phys. Rev. B **43**, 3337 (1991); J. Phys.: Condens. Matter **2**, 1593 (1990).
[22] K. Buchta, G. Fáth, Ö. Legeza, and J. Sólyom, Phys. Rev. B **72**, 054433 (2005).
[23] A. Läuchli, G. Schmid, and S. Trebst, cond-mat/0607173 (unpublished).
[24] D. Porras, F. Verstraete, and J. I. Cirac, Phys. Rev. B **73**, 014410 (2006).
[25] S. Tsuchiya, S. Kurihara, and T. Kimura, Phys. Rev. A **70**, 043628 (2004).
[26] S. R. White, Phys. Rev. Lett. **69**, 2863 (1992); S. R. White, Phys. Rev. B **48**, 10345 (1993).
[27] U. Schollwöck, Rev. Mod. Phys. **77**, 259 (2005).
[28] I. P. McCulloch and M. Gulácsi, Europhys. Lett. **57**, 852 (2002).
[29] See, for example, L. C. Biedenharn and J. D. Louck, *Angular Momentum in Quantum Physics* (Addison Wesley, Massachusetts, 1981).
[30] K. G. Wilson, Rev. Mod. Phys. **47**, 773 (1975).
[31] F. D. M. Haldane, Phys. Rev. Lett. **47**, 1840 (1981).
[32] F. Zhou, Europhys. Lett. **63**, 505 (2003).
[33] H.-J. Schmidt, J. Schnack, and M. Luban, Europhys. Lett. **55**, 105 (2001).